nuclear fusion
IAEA

PAPER • OPEN ACCESS

Overview of first JT-60SA plasma operation and plans in view of ITER and DEMO

To cite this article: J. Garcia *et al* 2026 *Nucl. Fusion* **66** 116011

OPEN ACCESS
IOP Publishing | International Atomic Energy Agency
Nuclear Fusion
Nucl. Fusion **66** (2026) 116011 (17pp)
https://doi.org/10.1088/1741-4326/ae74e1

Overview of first JT-60SA plasma operation and plans in view of ITER and DEMO

J. Garcia[1,a,*], M. Yoshida[2], H. Urano[2], K. Takahashi[2], S. Davis[3,b], V. Tomarchio[3], G. Phillips[3], T. Abe[2], N. Aiba[2], Y. Akazawa[2], M. Akimitsu[2], T. Ariizumi[2], K. Asakura[2], J. Ayllon-Guerola[4], A. Belpane[5], W. Bin[5], J. Buermans[7], A. Buzás[8], S. Cabrera[9], D. Carralero[9], L. Carraro[5], M. Cavinato[3], M. Cecconello[10], S. Chiba[2], S. Clement-Lorenzo[3], S. Coda[11], G. Cseh[8], A. Cubi[3], E. De la Luna[9], G. De Marzi[12], G. De Tommasi[13], M. Di Giacomo[3], F. D'Isa[5], Y. Endo[2], T. Estrada[9], M. Fabbri[3], G. Falchetto[1], A. Fassina[12], A. Ferro[5], C. Fiamozzi Zignani[12], T. Françonnet[3], G. Frello[3], K. Fukui[2], M. Fukumoto[3], E. Gaio[12], J. Galdon-Quiroga[4], Manuel Garcia-Muñoz[4], L. Garzotti[14], J. Gonzalez-Martin[4], K. Grodzicki[15], R. Guillén González[3], N. Hajnal[3], K. Hamada[2], K. Hamada[2], K. Hasegawa[2], S. Hatakeyama[2], V. Hauer[16], N. Hayashi[2], T. Hayashi[2], R. Heller[16], J. Hinata[2], S. Hiranai[2], J. Hiratsuka[2], H. Homma[2], H. Hurzlmeier[3], M. Iafrati[12], H. Ichige[2], M. Ichikawa[2], T. Iijima[2], R. Ikeda[2], S. Inoue[2], A. Isayama[2], T. Ishii[2], K. Ishita[2], E. Joffrin[1], A. Jokinen[3], K. Kajiwara[2], I. Kamata[2], A. Kaminaga[2], K. Kamiya[2], Y. Kashiwa[2], M. Kashiwagi[2], K. Kawano[2], T. Kawate[2], H. Kayano[2], Y. Kazakov[7], K. Kikuchi[2], K. Kimura[2], M. Kisaki[2], Y. Ko[2], T. Kobayashi[2], K. Kobayashi[2], K. Kobayashi[2], G. Kocsis[8], A. Kojima[2], S. Kojima[2], K. Kojima[2], M. Komata[2], K. Komuro[2], A. Kondo[2], R. Kurosawa[2], B. Lacroix[1], P. Lang[17], Q. Le Coz[1], R. Marques-Gomez[4], J. Martínez[9], R. Matoike[2], S. Matsuoka[2], Y. Miyata[2], Y. Miyo[2], K. Mogaki[2], P. Moreau[1], T. Morimoto[2], H. Murakami[2], M. Murayama[2], S. Nakamura[2], T. Nakano[2], S. Nemoto[2], C. Nguyen Thanh Dao[1], S. Nicollet[1], S. Nishimura[2], T. Nishiyama[2], M. Nocente[18], L. Novello[3], Y. Ohmori[2], Y. Ohtani[2], M. Ohzeki[2], J. Okano[2], Y. Onishi[2], C. Ortiz Ferrer[3], T. Oshima[2], A. Owada[2], R. Pasqualotto[5], E. Perelli[12], L. Pigatto[5], B. Plöckl[17], R. Prokopowicz[15], G. Pucella[12], G. Puglisi[3], D. Radloff[16], P. Rancsik[3], D. Réfy[8], A. Reyner-Viñolas[4], N. Richermoz[1], D. Rigamonti[6], E. Rosen[2], H. Saeki[2], H. Saeki[2], Y. Saito[2], S. Sakamoto[2], S. Sakata[2], R. Sakurai[2], L. Sanchis-Sanchez[4], R. Sano[2], T. Sasajima[2], H. Sasao[2], M. Sato[2], F. Sato[2], M. Sawahata[2], N. Seki[2], Y. Shibama[2], K. Shimada[2], J. Shinde[2], K. Shinohara[2], T. Shinya[2], S. Sonoda[2], C. Sozzi[6], H. Strobel[16], M. Sueoka[2], H. Sugiyama[2], A. Sukegawa[2], S. Sumida[2], T. Suzuki[2], S. Suzuki[2], M. Suzuki[2], M. Suzuki[2], M. Suzuki[2], T. Suzuki[2], L. Swiderski[15], Tamás Szepesi[8], J. Szewinski[15], S. Tadokoro[2], M. Takechi[2], K. Takeda[2], Y. Tanaka[2], M. Tardocchi[12], M. Terakado[2], B. Teuchner[3], H. Tobari[2], N. Toida[2], M. Tomine[2], A. Torre[1], T. Totsuka[2], K. Tsuchiya[2], D. Tsuru[2], K. Tyminska[2], D. Umezaki[2], S. Unno[2], J. Uno[2], K. Usui[2], M. Valisa[5], M. Márk Varga[8], M. Vavrik[8], L. Velarde-Gallardo[4], M. Verrecchia[3], R. Wada[2], T. Wakatsuki[2],

[a] Present address: Fusion for Energy, Garching, Germany.
[b] Present address: United Kingdom Atomic Energy Authority, Culham Campus, Abingdon, Oxfordshire OX14 3DB, United Kingdom of Great Britain and Northern Ireland.
[*] Author to whom any correspondence should be addressed.

M. Wanner[3], S. Watanabe[2], M. Wischmeier[19], R. Yaginuma[2], J. Yagyu[2], T. Yamamoto[2], S. Yamamoto[2], H. Yamanaka[2], K. Yamauchi[2], R. Yamazaki[2], H. Yamazaki[2], S. Yamoto[2], K. Yanagihara[2], K. Yanagihara[2], S. Yokooka[2], T. Yokoyama[2], N. Yoshizawa[2], L. Zani[1] and B. Zaniol[5]

[1] CEA, Saint Paul-Lez-Durance, France
[2] National Institutes for Quantum Science and Technology, Naka, Japan
[3] Fusion for Energy, Garching, Germany
[4] Universidad de Sevilla, Sevilla, Spain
[5] Consorzio RFX (CNR, ENEA, INFN, Università di Padova, Acciaierie Venete SpA), C.so Stati Uniti 4, 35127 Padova, Italy
[6] Institute for Plasma Science and Technology, CNR, via R. Cozzi 53, 20125 Milano, Italy
[7] Laboratory for Plasma Physics, LPP-ERM/KMS, Brussels, Belgium
[8] Fusion Plasma Physics Department, Centre For Energy Research, Konkoly-Thege Miklós út 29-33, Budapest, 1121, Hungary
[9] Laboratorio Nacional de Fusión, CIEMAT, Madrid, Spain
[10] Department of Physics and Astronomy, Uppsala University, SE-75120 Uppsala, Sweden
[11] Ecole Polytechnique Fédérale de Lausanne (EPFL), Swiss Plasma Center (SPC), CH-1015 Lausanne, Switzerland
[12] Dip.to Fusione e Tecnologie per la Sicurezza Nucleare, ENEA, C. R. Frascati, via E. Fermi 45, 00044 Frascati (Roma), Italy
[13] Dipartimento di Ingegneria Elettrica e delle Tecnologie dell'Informazione, Università degli Studi di Napoli Federico II, Napoli, Italy
[14] United Kingdom Atomic Energy Authority, Culham Campus, Abingdon, Oxfordshire OX14 3DB, United Kingdom of Great Britain and Northern Ireland
[15] IPPLM Association, Institute of Plasma Physics and Laser Microfusion, Hery 23, 01-497 Warsaw, Poland
[16] Karlsruhe Institute of Technology, Hermann-von-Helmholtz-Platz 1, 76344 Eggenstein-Leopoldshafen, Germany
[17] Max-Planck-Institut für Plasmaphysik, D-85748 Garching, Germany
[18] Dipartimento di Fisica 'G. Occhialini', Università di Milano-Bicocca, Milano, Italy
[19] EUROfusion Programme Management Unit, Garching bei Munchen, Germany

E-mail: Jeronimo.garcia@cea.fr

Received 26 January 2026, revised 15 May 2026
Accepted for publication 29 May 2026
Published 23 June 2026

Abstract

JT-60SA is the world's largest superconducting tokamak in operation jointly built and exploited by Europe and Japan in the framework of the Broader Approach. JT-60SA aims at addressing some of the technological and physics challenges, such as the long pulse steady-state plasma operation at high beta. The start-up of JT-60SA, which culminated in the first JT-60SA plasma achieved on 23 October 2023 and Operation-1 (OP-1) until the end of 2023, including the achievement of >1 MA diverted plasmas, paves the way for a new generation of large superconducting tokamaks, such as ITER. Several key scientific topics were investigated during this initial phase. Similarly to ITER, the available parallel electric field ($E_{\|}$) is low and yet plasma initiation was quickly obtained by means of the trapped particle configuration (TPC) with the assistance of $\sim$1.5 MW of electron cyclotron resonance heating (ECRH). A first analysis and classification of the causes for disruptions have been done after the results of OP-1. Vertical displacement events (VDEs) were responsible for the vast majority of disruptions in increasing elongated plasmas, as the stabilization plate was not yet installed in this phase. Therefore, VDE predictors and control algorithms were developed using machine learning techniques with magnetics probe data, showing that these novel techniques are also suitable for the start-up tokamak phases characterized by scarce input data. JT-60SA will restart

operation in 2026 following a series of upgrades. The experimental programme for future operations is guided by significant modelling 'predict first' activity, which shows that access to and development of H-mode in conditions of future burning plasmas will be possible with high negative neutral beam injection (N-NBI) and ECRH input power. The integration of such elements into a steady-state long pulse operation will be done with the installation of W plasma facing components (PFC) after the initial campaigns.

Keywords: tokamak, nuclear fusion, JT-60SA

(Some figures may appear in colour only in the online journal)

1. Introduction

JT-60SA is the largest superconducting tokamak in operation since the 23 October 2023, when the first plasma was produced. This achievement is a milestone of the JT-60SA project, which started in 2007 based on the agreement between EU and Japan for the joint implementation of the Broader Approach (BA) activities in the field of fusion energy research (BA Agreement) as well as Japanese domestic fusion research and development programme [1]. After 2007, the tokamak assembly started from 2013 and the assembly was completed in 2020. The Integrated Commissioning was conducted during the first plasma operation phase in 2020 and 2023 [2–4].

JT-60SA has three important missions, i.e. (i) addressing potential ITER related issues in advance while having the capability of optimizing ITER operation scenarios at break-even equivalent conditions, (ii) conducting complementary research to ITER, especially studying long pulse steady-state operation and related physics at high β_N and high performance plasmas for providing directions to the DEMO design activity, and (iii) fostering next generation scientists and engineers by building up their experiences through JT-60SA operation. In order to attain these goals, JT-60SA can develop high current, highly shaped plasmas with high heating by systems such as neutral beam injection (NBI) and electron cyclotron resonance heating (ECRH), which provide flexibility in terms of torque and electron to ion heating. A summary of the main characteristics of JT-60SA can be found in table 1 and a description about how the construction and development of the JT-60SA project has been shared between Japan and Europe is shown in figure 1.

The scientific exploitation of JT-60SA has been divided into different phases [5] as shown in table 2. JT-60SA entered into the start-up phase with the Initial research phase I by performing the integrated commissioning during 2020–2021 and 2023. This integrated commissioning had the goal to test the integrity of the machine to fulfil its scientific expectations and to provide a first set of scientific results that could be used to better prepare the following experimental campaigns. It is worth to point out that the start-up of a superconducting device of the JT-60SA size marks by itself an unprecedented achievement that can definitely contribute to the future start-up of other superconducting tokamak devices such as ITER.

Major goals of the JT-60SA integrated commissioning were to perform integrated test of the coils and to develop auxiliary plant control systems, including interlock systems, with the aim of ensuring a safe first plasma operation phase (OP-1). In such a phase, the scientific goals were to achieve a MA-class divertor plasma, demonstrate stable plasma control from current-up to ramp-down including ECRH assisted breakdown in low parallel electric field ($E_{\parallel}$) conditions, qualify wall cleaning and conditioning techniques, to provide a first assessment of disruptions and run-away electron (RE) generation and to provide a first evaluation of the plasma performance. All these goals were successfully attained during OP-1. Importantly, while most of the OP-1 was carried out using helium, hydrogen was also used to test breakdown and plasma development. Similar results were obtained in H compared to He, which ensures the robustness of the results obtained.

A particular important aspect has been the significant predict first modelling activity that has accompanied the preparation of OP-1 in order to guide and optimize the work to be done during the plasma phase development. Such a work has provided valuable information about how to speed-up some of the key research topics in OP-1, such as the plasma breakdown, which was obtained after just two days of operation. Therefore, the JT-60SA start-up paves the way to future large superconducting tokamaks, notably those generating significant fusion power, since they will have to rely on validated modelling to assess the plasma development prior and during their operation, as expected in ITER.

This paper is organized as follows. In section 2, the risk mitigation to avoid incidents in the coils as well as a brief explanation of the restart of the integrated commissioning in 2023 are reminded. In section 3, the main results of the integrated commissioning and OP-1 are described. In section 4, the status of JT-60SA, timeline and scientific priorities are shown. In section 5, the preparation for the scientific exploitation of the future campaigns within the experiment team (ET) is described. In section 6, the conclusions are given.

2. Risk mitigation strategy and restart of integrated commissioning

The JT-60SA tokamak has a full superconducting magnet system that consists of 18 toroidal field (TF) coils, four modules of

Table 1. Typical parameters of JT-60SA at nominal configuration [1]. B_t is the toroidal magnetic field. I_p the toroidal current. A is the aspect ratio. R and a the major and minor radius respectively. κ and δ are the elongation and triangulatiry respectively.

Magnitude	Value
B_t	2.25 T
I_p	5.5 MA
R/a ($A = 2.5$)	2.96/1.18 m
κ/δ	1.93/0.5
Flat top duration	100 s
Total power of negative N-NBI beams at 500 keV	10 MW
Total power of positive P-NBI beams at 85 keV	24 MW
Total ECRH power (82, 110, 138 GHz)	7 MW

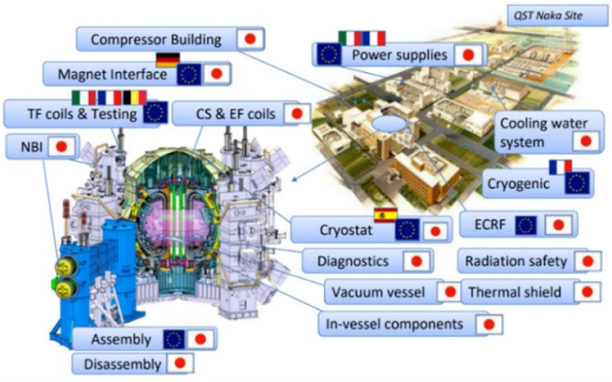

Figure 1. Origin of the different components used in the construction and upgrade of JT-60SA.

Central Solenoid (CS), and six circular equilibrium field (EF) coils [1, 2]. A series of measures were taken, before the integrated commissioning and OP-1 started, to reinforce the risk mitigation to avoid any incident with coils as the one reported in [2]. Such measures combined several safety approaches: (i) reinforcement of coil insulation, (ii) avoiding unnecessary voltage application to the coil systems, i.e. operation was carried out far from nominal coil limits, and (iii) immediate de-energization of the coils when vacuum condition deteriorates. A key activity carried out before plasma operation was the performance of local Paschen tests (LPTs) to verify the right coil insulation where reinforcement was conducted. Furthermore, global Paschen test (GPT) were also done to confirm the insulation performance of repaired joints, feeders and other electric circuits inside the cryostat. GPT was carried out at different cryostat pressures. Nevertheless, since reaching a condition of fully Paschen tight was unlikely, it was decided to proceed to the test phase once the inter-lock system, which quick ensures de-energization of the coils when vacuum condition deteriorates, was developed.

High Voltage tests of the superconducting coils were successfully performed in August 2023 and the energization of the TF and poloidal field (PF) coils was carried out including the validation of quench detector system in case the cryostat vacuum was degraded [6]. Such safety measures enabled the smooth progress of the integrated commissioning phase, the first plasma and the subsequent operation OP-1.

3. Main results from integrated commissioning and OP.1

The first plasma was obtained in OP-1 at toroidal current $I_P = 130$ kA and toroidal magnetic field $B_t = 2.0$ T while the whole OP-1 reached $I_P = 1.2$ MA plasmas in diverted configuration [3, 7]. The development of such initial plasmas has provided important information that is key for future devices such as ITER or DEMO in a number of important topics as describe in the following sections.

3.1. Plasma initiation

In JT-60SA the available parallel electric field ($E_{||}$) can be as low as 0.15 V m^{-1} and therefore the plasma initiation can be challenging if the usual field null configuration (FNC) approach is used [7]. This feature is common to those tokamaks using central superconducting solenoids such as in ITER and expected to be the case in DEMO. For instance, the inductive electric field in ITER is expected to be 0.3 V m^{-1}, which has been a matter for concern about its impact on the ITER start-up phase. While plasma initiation has been achieved in several tokamaks in FNC conditions at low $E_{||}$, the start-up phase of JT-60SA has provided a unique chance to extend previous studies to a large superconducting tokamak.

With the aim of analysing this issue before plasma operation, extensive simulations with the TOSCA code were carried out. It was found that the trapped particle configuration (TPC) technique assisted by ECRH could provide a better access to plasma initiation and following current ramp-up than the more typical FNC. Plasma initiation with TPC was tested and successfully led to the first plasma on the 23 October 2023 [7, 8]. The first plasma was obtained at $I_p = 130$ kA with a limiter configuration. Both fundamental resonance (82 GHz) and second harmonic resonance (110 GHz) ECRH were applied and positively tested during these discharges at a toroidal magnetic field of 2.0 T. The burn-through of the main gas (He) was clearly observed in both resonances. Importantly, the FNC start-up scenario, with the same prefill gas pressure than TPC,

Table 2. Summary of the initial research phase.

Research phase	Focus of exploitation	Operation Campaign		Divertor	Installed NBI power	Installed ECRH power	Max. usable aux. power
Initial research phase I	Integrated Commissioning	OP-1	H	Open upper inertially cooled carbon	0	1.5 MW (2 Gyro.)	1.5MW
	Initial stable and reliable operation • H operation for commissioning towards D operation. • Stable operation at high current heated plasma	OP-2		Lower pumped carbon with intershot cooling	P-NBI 8 units, plus N-NBI Total 16MW (with H) 23.5 MW (with D)	3 MW (4 gyro)	19MW
Initial research phase II	**ITER and DEMO regime access** • Access to ITER-relevant high confinement H-mode at high Ip • High beta access • ITER risk mitigation (ELM, disruption)	OP-3	D				26.5MW
		OP-4			P-NBI 12 units, plus N-NBI Total 30 MW		33 MW

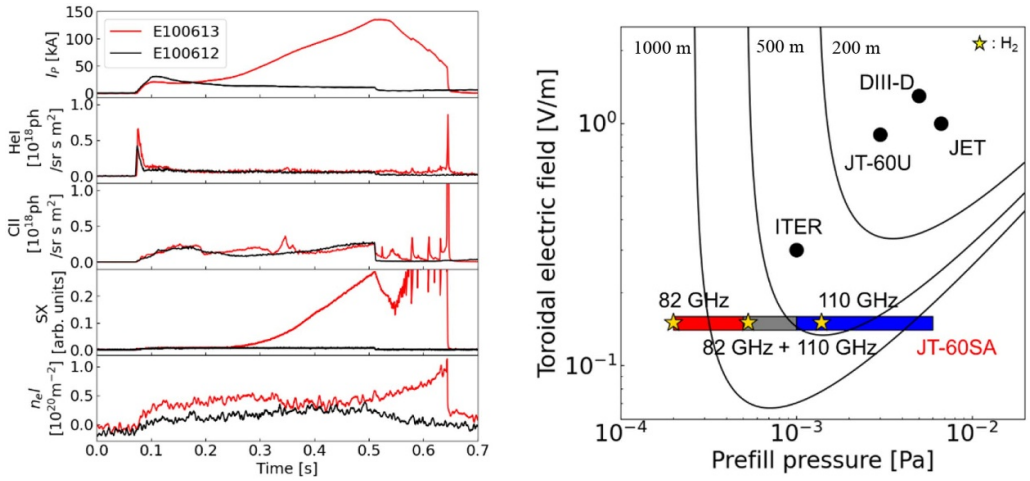

Figure 2. Comparison of discharge waveforms of initial trials of the TPC scenario (E100613, red) and the FNC scenario (E100612, black) (left). Prefill pressure and toroidal electric field operational parameter space for breakdown in JT-60SA with 82 GHz ECRH, 110 GHz ECRH and simultaneous injection. Operational ranges were examined using He prefill gas whereas successful H2 discharges were also demonstrated at operational points shown as stars. The minimum electric field required for Townsend avalanche breakdown for H_2 with connection lengths of 200 m, 500 m and 1000 m, and the typical operational points for JT-60U, DIII-D, JET and ITER, are shown for comparison (right).

failed under similar conditions, see figure 2 (left), which shows that TPC is more efficient than FNC in conditions of low $E_{\|}$. While most of the discharges during OP-1 were carried out in He, for minimizing wall recycling and speed-up the start-up, plasma initiation was also tested using H, achieving similar results.

A summary of the operational range for the toroidal electric field and the prefill pressure used during OP-1 in JT-60SA is shown in figure 2 (right). Importantly, breakdown was obtained in a wide range of prefill pressure at low toroidal electric field when including either first or second ECRH harmonics or a combination of both. Comparing these results to the typical operation point of JT-60U and other tokamaks with the one expected in ITER, JT-60SA has demonstrated breakdown at significant lower toroidal electric field. This achievement supports the expected development of the first plasma in ITER, as ITER is planned to initiate operation with half of its full toroidal magnetic field, utilizing second harmonic EC injection.

Throughout the first operation of JT-60SA, the effective use of ECRH proved critical to plasma start-up at low inductive electric fields, which was achieved in both FNC and TPC configurations. However, the EC-assisted FNC experiments revealed that this configuration was also highly sensitive to device model errors, which caused residual PFs and outward plasma displacement. In contrast, the TPC scenario enabled robust plasma position control owing to the finite vertical magnetic field applied during the whole plasma initiation phase.

3.2. Plasma Shape reconstruction and control

Once the breakdown is achieved, it is essential to ramp-up the plasma to higher current by keeping the plasma position and shape well controlled. This was done in JT-60SA by using several approaches for the plasma equilibrium reconstruction and the plasma shape control.

The position and last closed flux surface (LCFS) were reconstructed in real time by using a Cauchy condition surface (CCS) scheme, in which boundary integral equations are solved inside the LCFS using magnetic measurements [9]. Furthermore, a validation of the ITER real-time reconstruction algorithms for the plasma current, centroid position, boundary and for the poloidal beta has been performed using the data collected during OP-1. The requirements for the validation of the ITER plasma magnetic diagnostic algorithms are the following ones [10]:

- Regarding the plasma shape, the reconstruction error along the gaps should be less than 1 cm.
- The reconstruction error on the plasma centroid vertical and radial position should be less than 1 cm.
- The reconstruction error on the plasma current should be less than 1% if $I_p > 1$ MA, or less than 10 kA otherwise.
- The error on poloidal beta reconstruction should be less than $0.05 + 0.05\%$.
- Time resolution poloidal beta estimation during I_p quenches shall be 0.1 ms.

The accuracy of the reconstruction is evaluated against plasma equilibria computed with the CREATE-NL nonlinear code. Importantly, the ITER requirements for the estimation of the plasma current are met while this is not the case for the plasma centroid position and shape due to the small number of available flux loops and the absence of Mirnov coils which measure the normal component of the magnetic field [10].

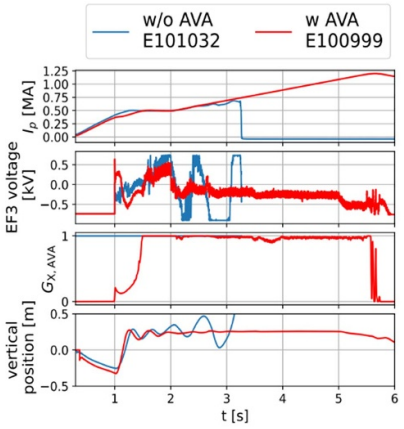

Figure 3. Comparison between the discharge E100999, using AVA, and E101032 without AVA. EF3 is the equilibrium field coil number 3. $G_{X,\mathrm{AVA}}$ represents the newly introduced gain in AVA to diminish the impact of I_p on power supplies control, and vice versa.

Predict-first modelling activity with the non-linear free boundary equilibrium code MECS [11] indicated potential poloidal coils voltage saturation when both the plasma current and shape changed at the same time, notably during the I_p ramp-up phase. This issue is a universal challenge in next-generation large-scale tokamaks, such as ITER and DEMO, which will be characterized by increase in inductance due to coil scaling, voltage saturation, and interference among multiple control objectives (current, position, and shape of plasmas).

The adaptive voltage allocation (AVA) scheme [12–14], which adaptively adjusts the balance between the position and shape control and the I_p control under the saturated power supply voltage condition, was developed prior to OP-1 using MECS and tested extensively during OP-1. AVA demonstrated a good performance during OP-1 as shown in figure 3. Without the AVA scheme, interference between different plasma control schemes lead to voltage saturation in the PF coils (+0.75/−0.90 kV in this phase), as exemplified by the EF coil number 3 (EF3) in figure 3, resulting in vertical position oscillations. By applying the AVA scheme, these oscillations were suppressed and plasma development up to $I_\mathrm{p} = 1.2$ MA was obtained [12, 13]. The results obtained are important since they demonstrate the capability of plasma shape and position control in DEMO relevant conditions with no stabilizing plate (SP) or in vessel coils as operated during OP-1. Nevertheless, the plasma shape and position control with AVA will be also demonstrated in more DEMO relevant plasmas, such as high beta plasmas, as expected to be developed in the following JT-60SA experimental campaigns.

These results highlight the importance of performing predict first simulations, in particular for plasma control, to ensure smooth and safe start-up phase of superconducting large tokamaks.

3.3. Vertical displacement events (VDEs) control

VDEs are one of the major concerns in the plasma development in large superconducting tokamaks as they can result in plasma disruption and machine damage. Therefore, the development of VDEs control is mandatory to safely conduct the start-up phase. During OP-1 in JT-60SA, VDE predictors and control algorithms were developed using machine learning techniques with magnetics probe data [15]. This is critical and highly relevant development for ITER and DEMO since it is done in a phase with few diagnostics available and scarce input data.

The VDE predictor and a direction control algorithm was developed using only magnetics probe data and a machine learning method called a Support Vector Machine (SVM). The SVM was trained with the discharge E101013, for which the elongation was artificially increased resulting in a highly negative decay index, defined as $n = -R/Bz\ \mathrm{d}Bz/\mathrm{d}R$ with Bz is a vertical magnetic field, vertical plasma displacement and vertical plasma velocity oscillations leading to an upward VDE as shown in figure 4. This behaviour is well predicted by the SVM model as shown in figure 4, in which the unstable vertical displacement region (VI) is depicted in red. The discharge E101013 clearly crosses the unstable region resulting in a naturally upward VDE in this upper null plasma configuration. The control was active in the equivalent discharge E101156, resulting in a positive plasma direction control by forcing a downward vertical displacement, allowing a good control of I_p as also shown in figure 4. This development is important since it can redirect the plasma into well protected machine locations. During OP-1, predictions were made using two variables. However, in preparation for OP-2, the system has been expanded to include multidimensional predictions with ten variables and significant improvements in prediction performance have been confirmed.

3.4. Plasma build-up and control

Once plasma initiation and control were demonstrated, scenario development was carried out in order to achieve ∼1 MA diverted plasmas. Such a development was useful to evaluate several parameters, e.g. magnetic flux consumption or plasma performance, before moving to the next phase. The data obtained is important as it allows the validation of codes that are used to assess and predict the next plasma operations.

Example of scenario development is the discharge E101162 [3] at $I_\mathrm{p} = 1.0$ MA with $B_\mathrm{T} = 2.04$ T, $R = 3.08$ m, $a = 1.28$ m, plasma ellipticity $\kappa = 1.49$ and triangularity $\delta = 0.39$, is given in figure 5. The strategy for such development was to use auxiliary ECRH power, ∼0.5–1 MW, to assist the ramp-up in order to minimize the magnetic flux consumption and to extend the plasma duration as much as possible. At $I_\mathrm{p} = 0.5$ MA, the transition from limiter to upper single null diverted plasma was established. The maximum duration of the $I_\mathrm{p} = 1$ MA flat-top with divertor configuration was about 3 s as shown in figure 5.

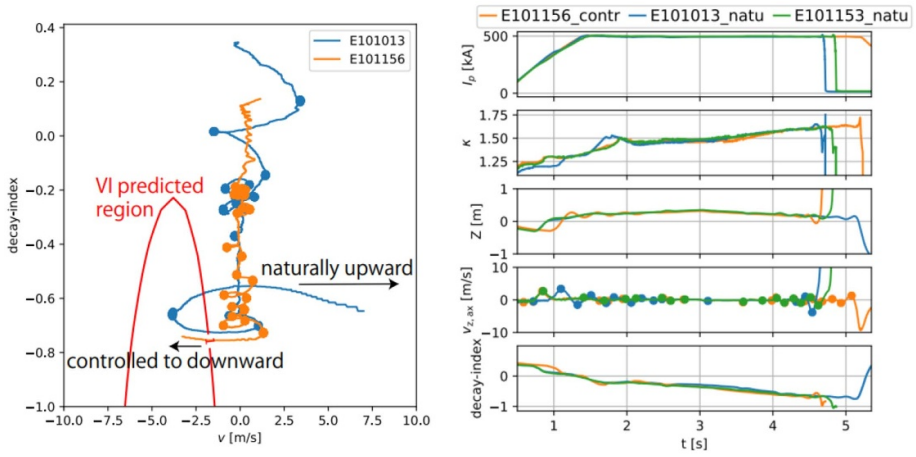

Figure 4. Machine learning VDE direction control demonstration for the discharge E101156 (left). Comparison between discharges with no VDE control (natural) and with VDE control (control) (right).

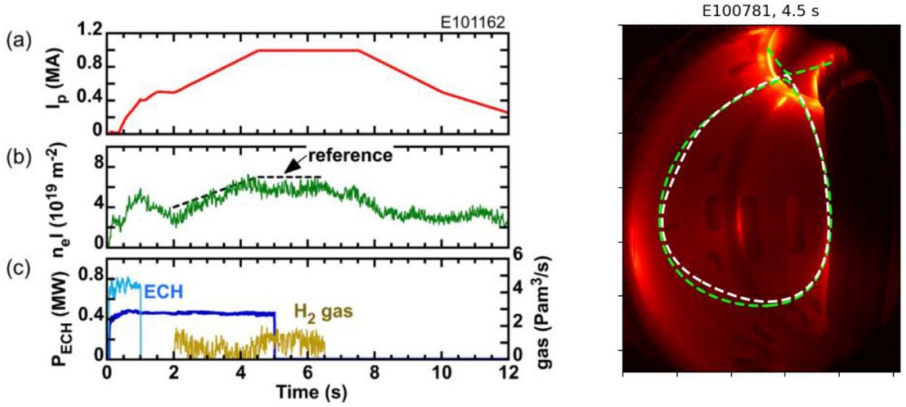

Figure 5. Main characteristics of the discharge E101162, which reached 1 MA including AVA control and density control. Reproduced from [3]. © IOP Publishing Ltd. All rights reserved. (Left). Image from the EDICAM camera in the visible spectrum for the discharge E100781. Reconstruction of the plasma equilibrium with CREATE-NL (white) and CCS (green) shows good agreement on the strike point location (right).

Importantly, the density control was also demonstrated during this phase as also shown in figure 5. The locations of the divertor strike points were confirmed by using the high-resolution visible camera, EDICAM [16] as shown in figure 5 and confirmed with divertor Langmuir probes and plasma equilibrium reconstruction. Stable plasmas at ∼1 MA with a few seconds flat top were obtained using both H and He gas. The experience obtained during this scenario development allowed to attain several unique achievements, such as the largest tokamak plasma volume, $V = 160$ m^3, and the highest toroidal current in a superconducting tokamak, $I_p = 1.2$ MA, which demonstrate that JT-60SA is ready to move to the following phase [14].

3.5. Disruption and RE generation

A first analysis and classification of the causes for disruptions have been done after the results of OP-1 [3, 17]. This is important because it is known that disruptions in the initial operation phase are due to the lack of maturity of the operation. Therefore, characterizing disruptions is important for speeding-up the learning curve of operations in future tokamaks such as ITER. In total 82 discharges disrupted out of 151 discharges in which the plasma shape and position were under control in the initial operation phase of JT-60SA. These 82 disruptions have been categorized into three classes according to their characteristics: VDEs, $n = 1$ magnetic perturbation and radiative disruptions.

VDEs were responsible for the vast majority of disruptions in increasing elongated plasmas [17], as the stabilization plate was not yet installed in this phase. Most of the disruptions with VDE origin were observed at $\kappa > 1.5$ with a clear impact of the gap between the plasma and the limiter as disruptions were likely to occur with lower κ when the gap became large, as reproduced with the MECS code. While MHD events have been observed, sawteeth and $n = 1$ tearing modes, a direct link to disruptions has not been established. Disruptions linked to the $n = 1$ perturbation mode were caused by the loss of controllability of the plasma shape and position when the mode was growing, rather than the impact of the mode itself. In such conditions, the plasma controller misinterpreted the plasma vertical position as unstable, even though the actual vertical

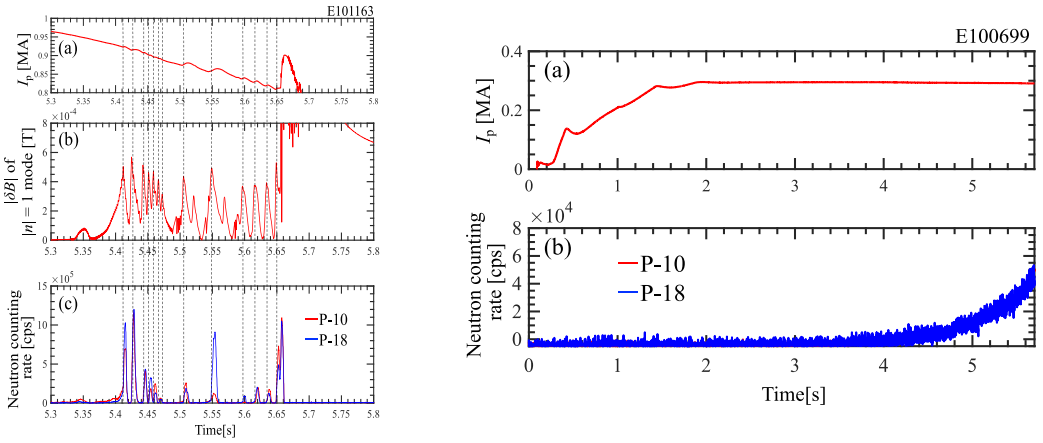

Figure 6. Time evolution of (*a*) I_p (*b*) the magnetic fluctuation amplitude $|\delta B|$ of the toroidal mode number $|n| = 1$ and (*c*) the neutron counting rates measured with NFMs at two positions in a typical discharge of the radiative disruption. (Left). Time evolution of (*a*) I_p and (*b*) the neutron counting rates measured with NFMs at two positions. The continuous RE loss is detected before the plasma disruption (right).

displacement of the plasma was small. Finally, radiative disruptions occurred in conditions of high neutral gas injection and edge cooling and/or ECRH auxiliary power removal.

Studying the generation of REs is essential as it is one of the main concerns of future tokamak devices with operational point at high I_p, such as ITER. REs can cause damage of plasma facing component (PFC) if they are not well controlled. Therefore, in JT-60SA, there has been a significant focus on analysing the cause of RE generation in the start-up phase of the device, which is crucial to predict RE behaviour when JT-60SA will reach its full operational capabilities [18]. Due to the lack of gamma diagnostics in OP-1, neutron flux monitors (NFMs) with ^{235}U fission chambers are used to indirectly detect the RE loss on PFCs via measurement of the photoneutrons generated by gamma rays impacting atoms in in-vessel components. This technique is useful as only Hydrogen and Helium gases, hence no fusion neutron products, were produced by the plasma.

Detection of REs is clearly linked to VDEs leading to disruptions as bursty signals of neutron counting rates are observed when the vibrated plasma hit the PFCs. Furthermore, a clear correlation between REs and the onset of $n = 1$ activity, caused by tearing modes, is detected. This is shown in figure 6, in which during the ramp-down phase of the discharge E101163, a clear correlation exists between the maxima of the fluctuating magnetic field caused by the $n = 1$ mode and the neutron emission peaks. Nevertheless, RE emission is also detected in non-disruptive plasma phases as also shown in figure 6 for the discharge E100699. In such a discharge, the neutron counting significantly increases at $t = 4.5$ s, which is linked to a growing RE beam at constant $I_p = 0.3$ MA and not associated to a VDE event or MHD activity. The physics mechanisms associated to this RE generation is the avalanche process.

Finally, an alternative methodology to assess RE generation was carried out by using the visible camera EDICAM, which is sensitive to high energy photons, hence it can be utilized for hard x-ray (HXR) dosimetry [19]. In case of high-energy photon—solid-state detector pixel interaction, photoelectrons are generated with significantly higher rate than for visible range photons. This results in a 'hot pixel' in the picture, having a significantly higher intensity than the neighbouring pixels. This feature enables the measurement of the high energy photon current quantitatively. This methodology has been applied to RE generation giving similar results to the one using neutron detector for the same discharges.

3.6. Confinement properties

Evaluating the thermal energy confinement properties of the initial JT-60SA plasmas and compare them to the expected confinement from well established scaling laws is essential to check whether the expectations are fulfilled. The energy confinement time obtained for JT-60SA L-mode diverted plasmas has been compared to the ITER96-P scaling [20] with the aim of evaluating whether the expected energy confinement time in ITER is obtained in OP-1 [21]. The plasmas within the database analysed are either ohmic or heated by ECRH using hydrogen. The global energy confinement time is evaluated from the energy balance equation ($\tau_E = W_{st}(P_{ECH}^{abs} + P_{OH} - dW_{st}/dt)^{-1}$) and from a transient analysis method by which a decay time of W_{st} after the ECRH stops is evaluated.

The energy confinement time is evaluated to be within 100 ms–200 ms as shown in figure 7. The results obtained highly depend on the confinement regime. A clear transition from linear ohmic confinement (LOC) to saturated ohmic confinement (SOC) confinement modes is observed depending on the electron density, with the LOC regime obtained at low densities. In general, in the first operation phase of JT-60SA, τ_E decreases with increasing total heating power and improves with rising average density $\bar{n}_e$. The global energy confinement

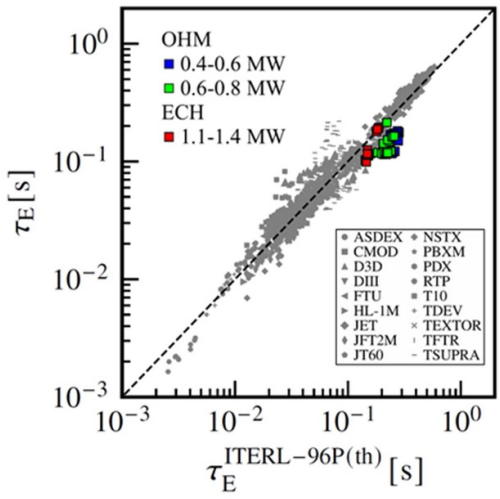

Figure 7. Comparison between the thermal energy confinement time found in OP-1 and the one derived from the ITER96-P scaling for several tokamaks.

time follows the neo-Alcator scaling [22] in the LOC regime, remaining below the ITER96-P scaling. At higher densities, the observed confinement characteristics suggest a transition toward the SOC regime, in which τ_E is expected to align more closely with the ITER96-P scaling. This is observed in figure 7, in which the discharges with τ_E close to the ITER96-P scaling are those at higher density in both ECRH and ohmic plasmas. Similar trends were also found when comparing to the ITER89-P scaling [23, 24]. These findings indicate that the confinement behaviour in JT-60SA plasmas is consistent with established scaling laws across different density regimes.

3.7. Wall conditioning

Electron cyclotron wall conditioning (ECWC) is considered for the inter-shot cleaning of the first walls in JT-60SA. During OP-1, a systematic study of ECWC with He gas was performed by changing the poloidal magnetic field pattern in TPC configuration and the ECRH conditions. Favourable conditions of the PF configuration and ECRH injections for H removal by ECWC were obtained [25]. In particular, the best results were obtained when He-ECWC plasma was produced on the inboard first wall where the start-up phase of the H tokamak plasma was produced. Nevertheless, the largest H removal rate was low, 1.0% after four tokamak discharges using H as a working gas. Further experiments will be carried out during OP-2.

3.8. Magnet and ECRH performance

As described in section 2, a series of measures were taken to avoid a potential incident in the JT-60SA coils as explained in [2] during the integrated commissioning and OP-1. Therefore, during OP-1 the current of PF coil was limited to 5 kA, which is 1/4 of the nominal current, and the magnetic flux that could be supplied was also 1/4 of the rated flux [26]. With these limitation, OP-1 was carried out with the aim of reaching 1 MA of plasma current. Finally, $I_p = 1.2$ MA was reached, which is roughly 1/4 of the maximum plasma current, $I_p = 5.5$ MA, established as a design target for JT-60SA. These results indicate that it is possible to reach a plasma current proportional to the amount of magnetic flux and therefore that JT-60SA may operate at its design targets in terms of plasma current in the upcoming experimental campaigns.

One key technical point that also significantly contributed to reach a maximum toroidal current of $I_p = 1.2$ MA during OP-1 was the good performance of the ECRH system, which was essential to develop the plasma breakdown. During the integrated commissioning phase of JT-60SA, two 1 MW gyrotrons were operated: unit 1, operating at 110 GHz and unit 2, able to operate at 82/110/138 GHz. The ECRH power is transmitted with high efficiency by the ∼100 m long transmission lines, achieving in the plasma experiment, a total of 1.51 MW of power from the two units [27]. After the first plasma, the ECRH system was used in almost all discharge sequences with a variety of injection configurations, demonstrating the reliability of this system. A source power of 1.5 MW at 110 GHz from a single unit (unit 2) was also tested and succeeded in 1 s injection. This result indicates the possibility of operating an ECRH system with a single-source power of 1.5 MW, which is an important achievement for future high-power operation in the following experimental campaigns.

4. Status of JT-60SA, timeline and scientific priorities

The JT-60SA current timeline of the initial research phase is shown in figure 8. By the end of 2025, JT-60SA is in the maintenance and enhancement phase 1 (ME1), while OP-2 will start in 2026. The JT-60SA project plan adopts a 'Phased Approach' with a gradual machine capability improvement, including diagnostics, in order to reach its highest performance and the main scientific goals, as shown in table 2 for the initial research phase I & II. The NBI and ECRH auxiliary power will be increased step by step, which will allow to access high performance at high density and I_p. In this initial phase, carbon PFCs are installed including an inertially cooled divertor. The initial research phase I & II will serve as a step ladder preparation for the extended research phase, which will be characterized by W PFCs and actively cooled divertor (ACD) in W, allowing the development of long pulse plasma operation at high β_N in a metallic environment as expected in DEMO. A summary of the main scientific priorities for each scientific campaign is shown in table 3. In the upcoming sections, the details of each phase will be described.

4.1. Maintenance and enhancement phase 1 (ME1)

After the successful integrated commissioning and OP-1 [3, 4], JT-60SA entered the ME1 phase [28]. JT-60SA is upgraded with new ports to allow high auxiliary heating power operation with 23.5 MW, including 10 MW of negative NBI (N-NBI) at 500 keV, and 3 MW of ECRH. Inertially cooled carbon divertor with divertor cryopump installed to allow heat flux of

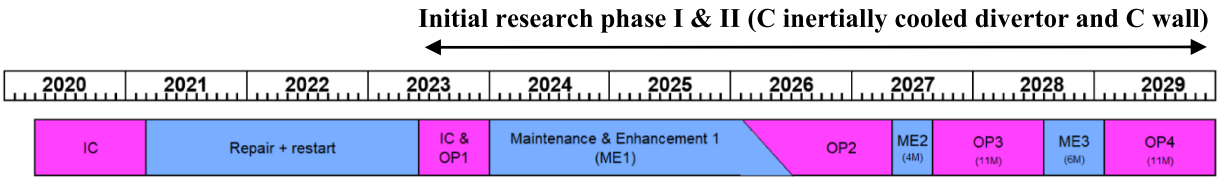

Figure 8. Overview of the timeline for operation (OP) and maintenance and enhancement (ME) phases.

Table 3. Summary of the scientific priorities for the different experimental campaigns in JT-60SA.

Initial research phase I & II (C inertial divertor and C wall)			Integrated research phase (W actively cooled divertor and W wall)
OP-2 (P_{aux} = 26.5 MW)	OP-3 (P_{aux} = 26.5 MW)	OP-4 (P_{aux} = 33 MW)	OP-5- (P_{aux} = 41 MW)
Stable operation at high current heated plasma	High confinement H-mode plasmas at high current including ELM control	Disruption mitigation and avoidance at high current in H-mode	Long pulse operation in W environment
H-mode access and characteristics	Physics of energetic particles	Heat load to divertor mitigation	
First high beta plasma attempt	Study of high beta plasmas	High beta plasmas compatible with radiative divertor	

10 MW m^{-2} for ∼5 s and 15 MW m^{-2} for ∼3 s. The SP with full carbon armours are set up in the torus direction, and behind the SP, in-vessel coils such as fast plasma position control coil (FPPCC) [29], error field correction coils (EFCC) and resistive wall mode control coils (RWMCC) are also installed. The massive gas injection (MGI) system is also installed, which will be essential for disruption studies. A summary of these upgrades installed during ME1 and the comparison with respect to OP-1 is shown in figure 9.

Specific work is being done during ME1 in order to ensure nominal operation in the upcoming experimental campaigns, notably concerning the coil current. The following actions have been taken [28]:

— Enhancement of insulations of joints and He inlets of EF coils.
— *In-situ* insulation reinforcement of He inlets/outlets on CS modules.
— Revised the controller of the quench detection (QD) system.
— Installation of the cold cathode gauges (CCG).

Most of the diagnostic systems, both from Japan [30] and EU [31] will be installed during ME1 for the use during OP-2: Thomson scattering system, vacuum ultra violet (VUV) divertor spectrometer, infrared TV camera system, ECE diagnostics system, CXRS diagnostics system, MSE polarimeter system, neutron profile monitor system, tracer-encapsulated solid pellet system. Specific agreements with General Atomics (GA) and Princeton Plasma Physics Laboratory (PPPL) were established in order to install the Fast Ion D-alpha (FIDA) diagnostic system, by GA, and x-ray imaging crystal spectroscopy (XICS) by PPPL.

4.2. OP-2 priorities

During OP-2, due to the installation of many new components and systems in ME1, there will be an integrated commissioning with and without plasma. At the beginning of OP-2, hydrogen operation is developed in order to avoid too much neutron generation and machine activation and hence most of the commissioning will be done in the hydrogen operation. Thereafter, deuterium operation starts as shown in table 2.

The scientific priorities to be developed during OP-2 will be in line with the new machine capabilities after the installation of new components and diagnostics and with the integrated commissioning items to be performed in hydrogen. As an example, this is the case of the commissioning of the N-NBI, which will include the increase in beam energy and power. The commissioning phase will support studies of shine-through and fast ion behaviour of the N-NBI, which is essential information for ITER. The use of hydrogen also allows for dedicated experiments profiting the change of isotope. This is the case of the L–H transition differences in hydrogen and deuterium, which can be very well characterized at this stage. For that purpose, the use of ECRH, N-NBI and P-NBI will provide essential information, as it will help to study the impact of electron vs ion heating and the impact of rotation in the L–H transition.

An important activity will be devoted to the tests and development of plasma control schemes, breakdown, error field and plasma formation studies. This is essential for providing stable plasmas for performing reliable experiments. The control schemes will be tested at different I_p, which will be gradually increased with the aim of reaching its maximum capability, i.e. 5.5 MA in L-mode. However, as typically happens in the

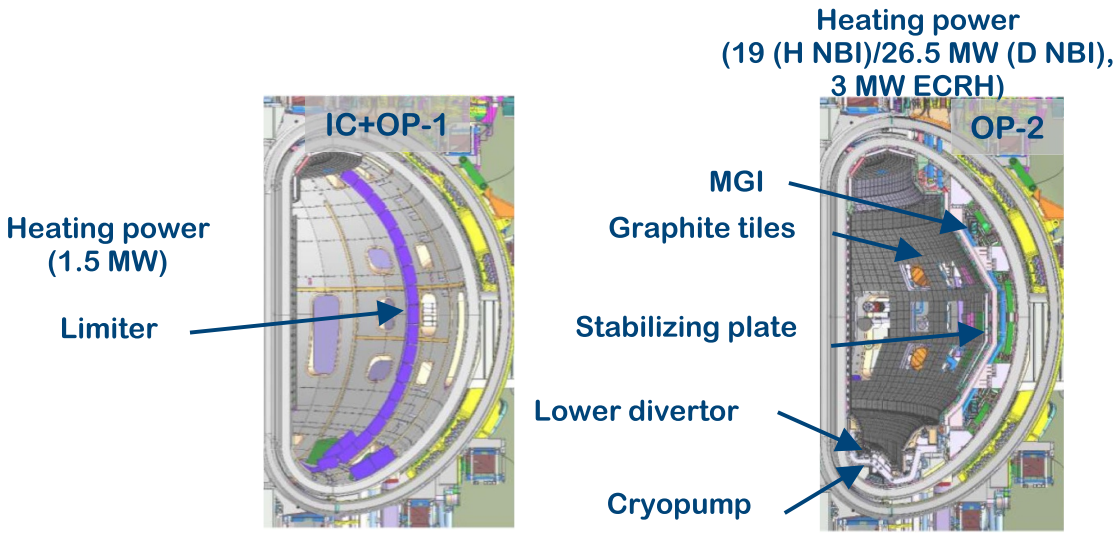

Figure 9. Main upgrades from OP-1 (left) being installed during ME1 for operation in OP-2 (right).

initial phases of any tokamak device, disruptions are expected as the current is increased towards the goal of 5.5 MA, therefore disruption studies including disruption mitigation studies with MGI will be a priority at high current in L-mode after a phase of commissioning of the MGI system. In this framework, the generation of runaway electrons is also expected and studies towards the understanding of their mitigation will be also important in ITER. A key element in which JT-60SA can provide key results from this initial phase is the scrape-off layer (SOL) scaling at high I_{p}, which is a matter of concern for ITER.

All the previous points are necessary steps to proceed towards the development of the demonstration of ITER-relevant H-mode plasmas which will be a priority in OP-2 as discussed in section 5.1.

4.3. OP-3 and OP-4 priorities

It is expected to achieve higher input power in OP-3 and OP-4 after all the commissioning and conditioning of NBI during OP-2 and the work to be done in ME2 and ME3. This will allow the consolidation of the entry to H-mode plasmas in the ITER-relevant scenario with type-I ELMs, including well established disruption mitigation with MGI at high current in H-mode, but also the development of plasmas at higher beta, hybrid and internal transport barrier (ITB) scenarios, which is a goal towards the demonstration of DEMO relevant scenarios. Access to higher beta naturally means that the scope of the experiments to be performed can be much wider. For example, there will be a special focus on advanced real time control techniques, RWM studies, neoclassical tearing mode (NTM) control, interplay between fast ions and turbulence, type-I ELMs formation, plasma regimes with small or no ELMs, and transport and turbulence studies. Since the range of beta achievable by JT-60SA is high, above the no wall limit, such studies can indeed provide high impact information.

One key element to be considered in this phase is the compatibility of high beta plasmas at high power with heat flux limitations to the inertially cooled divertor. Specific techniques to make compatible high beta studies and divertor limitations will be tested, in particular, impurity seeding and impurity transport studies will be carried out as a preparation for the integrated research phase.

4.4. W-PFC transition

At the end of the initial research phase, it is expected a transition to the integrated research phase with a change from C-PFCs to W-PFCs including an ACD and the increase of NBI power up to 34 MW and ECRH up to 7 MW. The installation of an ACD will allow to develop long pulse operation in order to study DEMO relevant plasmas in particular steady-state regimes at high β_{N}. Furthermore, the installation of W-PFCs also expands the scientific scope of JT-60SA towards W-related ITER relevant scientific topics after its rebaseline [32]. Scientific topics such as the compatibility of steady-state plasma regimes at high β_{N} in a metallic environment, the source of W at high input power conditions, the possibility of W screening and its control at the plasma edge or the W migration and redeposition will be studied in a metallic environment and in long pulse operation. Such results will expand current studies about long pulse operation in metallic environment, such as the ones developed in WEST [33] and EAST [34], towards high input power and high current.

R&D of the high heat flux (HHF) components of the ACD in W is on-going. They will allow heat flux of 10 MW m^{-2} for 100 s. In the present plan, the ACD is planned to be installed after OP-4, because much more time is needed to install the ACD comparing with the period of time for maintenance & enhancement: ME2 (4 months) and ME3 (6 months).

Table 4. Expected plasma scenarios to be developed in OP-2.

	I_p/B_t (q_{95})	β_N/β_P	H_{98} (y,2)	n_{GW}
OP-2 baseline	4.6 MA/2.28 T ($q_{95} \sim 3$)	$\sim 2/< 1$	~ 1	0.4–0.6
OP-2 hybrid	2.7 MA/1.70 T ($q_{95} \sim 4$)	~ 2–$3/\sim 1$	>1.1	>0.4
OP-2 ITB	1.7–2.0 MA/1.70 T ($q_{95} > 6$)	$>3.5/\gg 1$	>1.2	>0.5

5. Preparation for the scientific exploitation within the JT-60SA ET

The JT-60SA scientific exploitation is managed under the so-called ET [2], which is composed of three experiment leaders (ELs), two from Japan and one from Europe, the topical group leaders (TGLs) and the participating researchers. The ET has been focusing in the last two years on the preparation of the initial JT-60SA campaigns with the aim of expanding the general research activities described in the JT-60SA research plan. A particular focus has been put on the use of predict first modelling activity to assess the research items expected to be developed in the initial research phase I & II, especially for OP-2. In particular, this activity has been carried out for scenario prediction for OP-2, which will start at limited input power of 19 MW in hydrogen and 26.5 MW in deuterium. Nevertheless, other important modelling predict first activities, including projections of W behaviour in JT-60SA, have been also carried out in view of a better definition of the experimental programme. Some of the activities are described in the following paragraphs.

5.1. Scenario preparation and prediction for OP-2

The target high confinement H-mode scenarios expected to be developed in OP-2 were established and initially explored with the ACCOME [35], METIS [36] and MECS codes considering the fact that limited auxiliary power will be available in OP-2. The main characteristics of these target scenarios are shown in table 4. These studies complement previous studies performed for the development of the main JT-60SA scenarios considering maximum machine capabilities [37–39].

An integrated simulation encompassing core-pedestal-SOL/divertor regions was performed to assess the H-mode scenarios shown in table 4 for the JT-60SA initial research phase [40]. The integrated modelling consists of a core transport simulation code GOTRESS+ [41] with the mixed Bohm-gyroBohm model [42] for turbulent transport, the EPED model for the pedestal characteristics [43], the Saarelma's density pedestal model [44], and a SOL/divertor simulation code SONIC [45, 46]. The scenarios investigated are the baseline with $B_t = 2.28$ T, $I_p = 4.6$ MA, $\kappa = 1.85$, $\delta = 0.5$, the safety factor at the 95% poloidal flux surface $q_{95} \sim 3.0$, the total auxiliary power $P_{aux} = 19$ MW in deuterium and the hybrid scenario at $Ip = 2.7\ MA$ and $Bt = 1.7\ T$, with $P_{aux} = 16.5\ MW$, and $\kappa = 1.8$, $\delta = 0.51$. For the baseline scenario, the L–H power threshold, P_{LH}, predicted by ITPA08 scaling is 8.54 MW with Greenwald fraction, $n_{GW} = 0.7$, meaning that $P_{aux} = 19$ MW is more than twice of P_{LH}. Using this approach, simulations results show that it is possible to obtain the expected performance of baseline scenario, i.e. $\beta_N \sim 2$, H_{98} (y, 2) ~ 1, in OP-2 conditions. Importantly, when using only deuterium neutral gas at a rate $\Gamma_{puff} = 1.0 \times 10^{21}$ s^{-1}, the outer divertor is in an attached condition, resulting in the peak heat load of $q_{\parallel} \sim 10$ MW m^{-2} with electron separatrix density $n_{e,sep} = 2.9 \times 10^{19}$ m^{-3} and $Z_{eff} \sim 1.4$. In order to reduce the heat load to the divertor, Ne is used as an extrinsic impurity, obtaining T_e less than 5 eV near the strike point, meaning that a partially detached condition was achieved with the peak heat flux of 6.2 MW m^{-2}, $n_{e,sep} = 2.5 \times 10^{19}$ m^{-3} and $Z_{eff} \sim 3.4$. As shown in figure 10, when using Ne, core pressure reduction is observed due to the increase in radiation power inside the separatrix by $\sim$2.8 MW. Nevertheless, in both with and without Ne puffing, the typical values of baseline scenario are obtained, confirming that the baseline scenario can be studied in OP-2. For the hybrid scenario, simulations show that stationary plasma conditions, with $q_{\parallel} < 10$ MW m^{-2}, can be achieved without extrinsic impurity injection by optimizing the deuterium fuelling rate as shown in figure 10. Importantly, the hybrid scenario show impurity screening of carbon in the pedestal region. This is shown in figure 10(c) for the carbon ionization state C^{6+} for which an outward neoclassical velocity pinch, positive $v_{C^{6+}}$, is obtained close to the separatrix. Therefore, JT-60SA will allow for edge impurity screening studies starting from OP-2.

The possibility of developing the hybrid scenario, $q_{min} \sim 1$, $\beta_N \sim 3$, $\beta_p > 1$, has been also studied with the JINTRAC [47] suite of codes after first simulations carried out with the METIS code [48]. Two versions of the hybrid scenario, $I_p = 3.7$ MA, $B_t = 2.28$ T and $I_p = 2.7$ MA, $B_t = 1.70$ T, with $P_{aux} = 19$ MW, were considered with the aim of maintaining q with a low magnetic shear region, $q_{min} > 1$ and low shine-through losses. The role of the off-axis current drive on maintaining $q_{min} > 1$ was particularly addressed. The results suggest that a high β_N ($\sim$3) regime with a high non-inductive current fraction ($\sim$70%) could be achieved during the initial research phase at 2.7 MA/1.70 T and at $f_{GW} = 0.4$. The role of NBI and neutral beam current drive (NBCD) and ECRH electron cyclotron current drive (ECCD) on shaping the q profile was specifically assessed. While both NBI heating and ECRH significantly contribute to the off-axis heating, the impact of ECCD is nearly negligible compared to the NBCD as shown in figure 11. Specifically, the contribution of the N-NBI to the NBCD is quite strong and controlling the current drive from NBI, notably the current provided by the N-NBI, is essential to avoid strong q profile reversal as shown in figure 11.

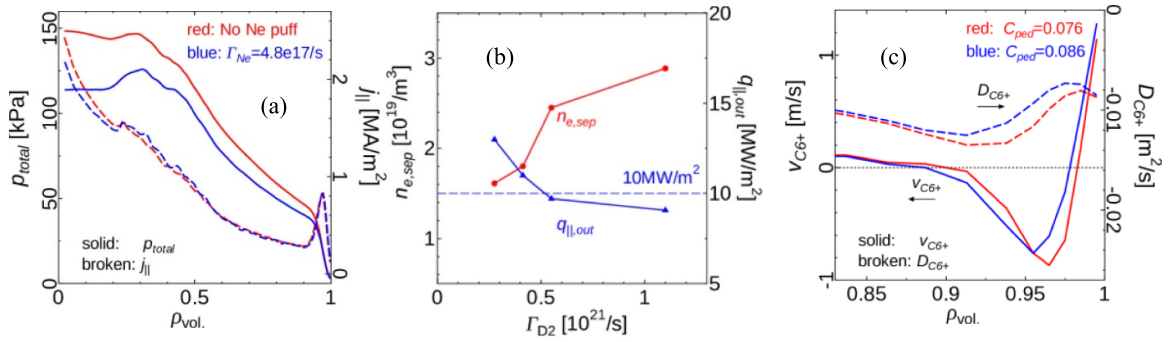

Figure 10. Differences in plasma pressure with only C injection or by adding Ne injection for the baseline scenario in OP-2 (*a*). Dependence of $q_{||}$ and $n_{e,sep}$ on Γ_{D2} for the hybrid scenario in OP-2 (*b*) Neoclassical particle diffusivity $D_{C^{6+}}$ and the convective velocity $v_{C^{6+}}$ for C^{6+} in the case of the hybrid scenario for OP-2. C_{ped} represents different assumptions for the EPED model as described in [39] (*c*).

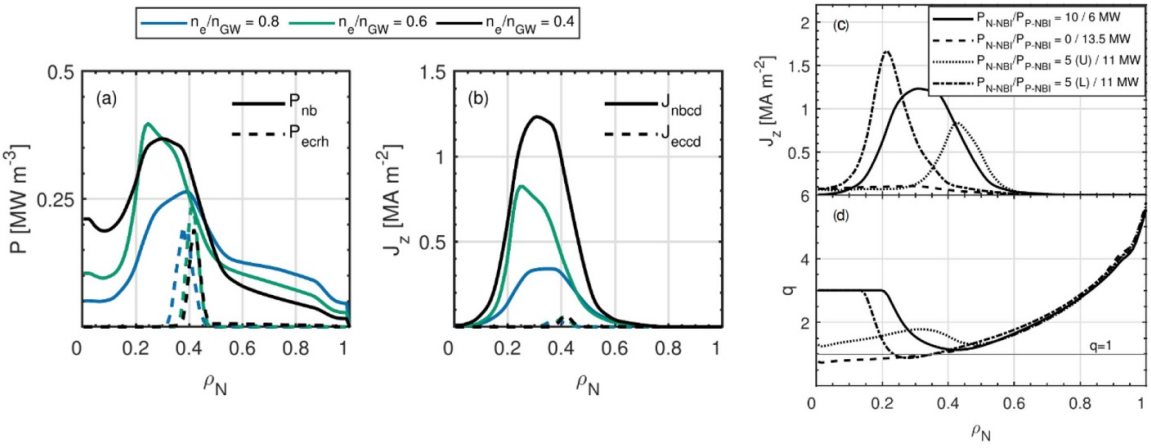

Figure 11. Auxiliary power density profile from NBI and ECRH for the hybrid scenario in OP-2 (*a*) auxiliary current drive density profile from NBI and ECRH for the hybrid scenario in OP-2 (*b*) current drive (*c*) and q (*d*) profile obtained at different combinations of N-NBI and P-NBI for the hybrid scenario. Reproduced from [48]. The Author(s). CC BY 4.0.

Finally, a special effort is done to develop tools able to prepare plasma discharges before the operation in order to minimize risks and prepare ITER operation, in which such tools will be essential. Pulse Design Simulator (PDS) tools such as the one based on METIS + NICE [49] or MECS have been validated with OP-1 experimental data and are being prepared for OP-2. PDS is capable of simulating a discharge from plasma breakdown to the very end of the discharge going through the start of ramp-up plasma, *X*-point formation, current flat top right to the ramp-down and include heating and transient phases with simplified models for the core response.

5.2. Fast ion, alpha particle and turbulence studies

JT-60SA has strong heating system flexibility. Notably its N-NBI will provide 10 MW of heating power with energy beam up to 500 keV. This feature will allow detailed fast ion studies during the initial research phase [50], such as the destabilization of fast ion related instabilities [51], the analysis of the fast ion generation and losses or the interplay between fast ions and thermal turbulence as it is expected from other large tokamaks, such as JET, in which a clear turbulent transport reduction is obtained in the presence of instabilities driven by highly energetic ions [52–56]. Turbulence in the presence of fast ions has been studied in JT-60SA by performing GENE [57] simulations of the scenario 3 from [5] at 41 MW of auxiliary power [58]. A clear interplay between turbulence and fast ion modes was found in electromagnetic simulations, which led to thermal fluxes oscillate with the high frequency of the fast ion driven modes. While thermal turbulent fluxes are generally low and the energy is mainly transported by the fast ion species, as shown in figure 12, they are quite sensitive to the specific thermal plasma background and the thermal fluxes can transit to the non-zonal transition (NZT), where zonal-flow-based saturation is disabled due to enhanced magnetic stochasticity at high $\beta_e \sim 2.7\%$ and/or profile gradients.

As of 2025, deuterium–tritium plasmas are not planned in JT-60SA. However, the fusion reaction $D_{beam} + {}^3He \rightarrow {}^4He$ (3.6 MeV) + p (14.7 MeV), which has its maximum cross-section close to 500 keV for fast deuterium, has been envisaged to study alpha particle production [59]. By using the Monte-Carlo code ASCOT [60], it is found that at 10% ^{3}He concentration and with 10 MW of N-NBI power, $\sim 8 \times 10^{16}$ s^{-1} alpha particle birth rate is obtained, four times higher than the JET equivalent results at 20%–25% concentrations of ^{3}He although at reduced NBI power (7 MW) [61, 62]. The slowed down

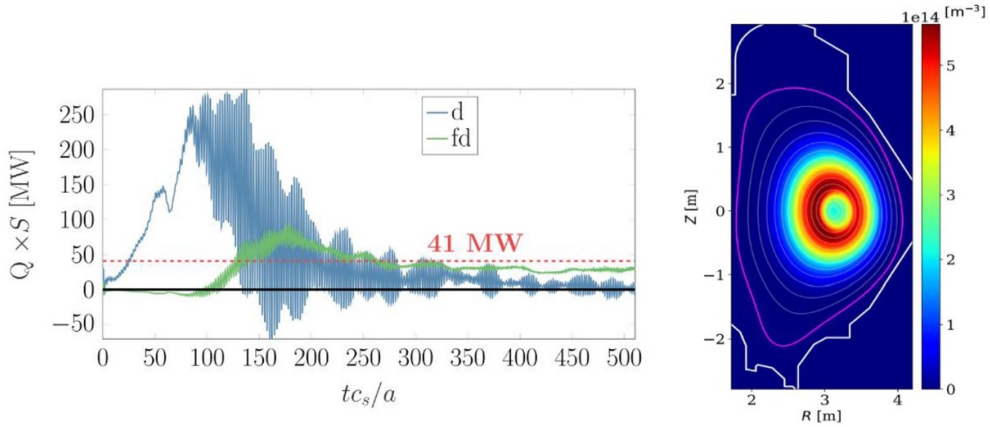

Figure 12. Deuterium and fast deuterium heat fluxes obtained from GENE simulations. Reproduced from [58]. The Author(s). CC BY 4.0., with the permission of IOP Publishing (left). Slowed-down alpha particle poloidal distribution as obtained from the ASCOT code (right).

alpha distribution is slightly off-axis, as shown in figure 12, due to the off-axis N-NBI deposition. The impact of MHD on alpha particle losses or the non-linear interplay between alpha particles and MHD modes in conditions of high $q_{\min}$ or reversed shear q profile driven by N-NBI can be investigated. This is an important information for steady-state plasma scenarios in D–T in ITER and DEMO, which might be characterized by low or even negative magnetic shear.

5.3. Plasma edge and divertor studies towards W operation

Long pulse operation at high beta, auxiliary power and plasma current will be the main characteristic of JT-60SA. Therefore, integrated power and particle exhaust scenarios represent a key element in operating the machine in safe conditions. This is particularly important when transiting to W-PFCs, in which potential W pollution of the plasma core by sputtering might limit the plasma performance. Several modelling studies have been carried out with the codes SOLPS-ITER [63] and SOLEDGE3X [64] in order to evaluate the controllability of the heat and particle flux to divertor in conditions of high auxiliary power. Simulations with SOLEDGE3X show that at an intermediate edge power of 15 MW in the scenario with $I_p = 5.5$ MA, $B_t = 2.25$ T and $P_{aux} = 30$ MW, there is a need for impurity injection during the first period of exploitation of the machine as 10 MW m^{-2} is obtained in attached cases, and achieving detachment is challenging, requiring upstream electron densities at least above 4×10^{19} m^{-3}. By using Ne seeding, it is shown that at 15 MW of power injected into the edge plasma, the inner target is easily detached and presents low heat loads. Therefore, JT-60SA will probably need to be operated in a deep detached regime in its first phase of exploitation for discharges longer than a few seconds. These results are similar to those obtained using SOLPS-ITER which in addition shows that the V-shaped outer divertor corner, designed to favour the detachment at low midplane plasma density, is particularly effective in trapping neutral particles in the corner, thus enhancing the momentum loss in the strike point region. The influence of these results on plasma operation when W divertor will be installed is being modelled in parallel to studies about potential optimized W divertor geometry and cooling system [65, 66].

6. Conclusions

After the construction phase, JT-60SA has entered into the initial research phase I by performing an integrated commissioning in 2023, which included significant amount of plasma operation and scientific development during OP-1. Several key results relevant for ITER and DEMO have been obtained in this initial phase. Plasma initiation was obtained in low $E_\parallel$ conditions as expected in ITER by using the novel TPC technique, which was extensively prepared before operation. Plasma position and shape control has been obtained by using the AVA scheme, which allows simultaneous control of plasma shape and I_p in conditions of saturated power supplies. Disruption and RE characteristics in the machine start-up phase were obtained. Such achievements allowed JT-60SA to enter into the MA-class tokamaks with a maximum I_p current of 1.2 MA in diverted plasmas, hence becoming the largest tokamak in operation.

JT-60SA is currently in a phase of maintenance and enhancement in which important upgrades, such as the lower inertially cooled divertor in C with cryopump, the NBI heating, in vessel coils and a large number of diagnostics are being installed to resume operation in 2026. Three campaigns will be developed using C-PFCs, in which essential scientific topics, such as L–H transition, scenario development at high current and density and performance, high β_N scenarios, plasma wall interaction and ELM control or disruption mitigation and prediction, will be explored. After these campaigns, a transition to W-PFCs, with an actively cooled divertor, is expected. The compatibility of long pulse steady-state plasma operation in high beta conditions, as expected in DEMO, will be a priority.

In the speedy development of plasmas during OP-1, the role of predict first modelling activities has been essential. The same type of activity has been followed to assess priority scientific items for OP-2. The results show that the development

of plasma scenarios in H-mode at high performance and I_p is possible in D, notably in conditions of high electron heating and low rotation, as expected in ITER.

Finally, the start-up of JT-60SA marks a landmark as it shows the importance of new techniques, such as predict first modelling or machine learning in conditions with scarce input data, to guide the operation and scientific development of a new large superconducting tokamak. The lessons learned are essential for the new generation of researchers that will certainly be fostered in the scientific exploitation of a large superconducting machine within the JT-60SA project before ITER and DEMO operation.

Acknowledgment

JT-60SA was jointly constructed and is jointly funded and exploited under the Broader Approach Agreement between Japan and EURATOM.

ORCID iDs

J. Garcia 0000-0003-0900-5564
M. Yoshida 0000-0002-2899-1323
H. Urano 0000-0001-8740-8954

References

[1] Kamada Y., Di Pietro E., Hanada M., Barabaschi P., Ide S., Davis S., Yoshida M., Giruzzi G. and Sozzi C. (JT-60SA Integrated Project Team) 2022 *Nucl. Fusion* **62** 042002
[2] Shirai H. *et al* 2024 *Nucl. Fusion* **64** 112008
[3] Yoshida M., Wakatsuki T., Urano H., Inoue S., Fukumoto M., Nakano T., Ohtani Y., Sano R., Yokoyama T. and Szepesi T. 2025 *Plasma Phys. Control. Fusion* **67** 065010
[4] Takahashi K. *et al* 2025 *Fusion Eng. Des.* **216** 115059
[5] JT-60SA research plan—version 4.0 (available at: www.jt60sa.org/wp/wp-content/uploads/2021/02/JT-60SA_Res_Plan-5.pdf)
[6] Yamauchi K., Hatakeyama S., Okano J., Ohmori Y., Terakado T., Shimada K., Frello G. and Novello L. 2025 *Fusion Eng. Des.* **216** 115091
[7] Wakatsuki T. *et al* 2024 *Nucl. Fusion* **64** 104003
[8] Wakatsuki T. *et al* 2026 Development of Low Inductive Electric Field Plasma Start-up in JT-60SA *Nucl. Fusion* accepted
[9] Miyata Y., Suzuki T., Fujita T., Ide S. and Urano H. 2012 *Plasma Fusion Res.* **7** 1405137
[10] Fiorenza F. *et al* 2026 *Fusion Eng. Des.* **222** 115486
[11] Miyata Y., Suzuki T., Ide S. and Urano H. 2014 *Plasma Fusion Res.* **9** 3403045
[12] Inoue S., Miyata Y., Urano H. and Suzuki T. 2021 *Nucl. Fusion* **61** 096009
[13] Inoue S., Miyata Y., Kojima S., Takechi M., Sano R., Wakatsuki T., Urano H., Yoshida M. and Suzuki T. 2025 *Nucl. Fusion* **65** 056020
[14] Inoue S. *et al* 2025 Development of equilibrium control simulator and experimental validation of advanced iso-flux equilibrium control during the first operational phase of JT-60SA *Preprint: 2025 IAEA Fusion Energy Conf.* (*Chengdu*) (available at: https://conferences.iaea.org/event/392/papers/35767/files/13382-mytemplate.pdf)
[15] Inoue S., Kojima S., Miyata Y., Wakatsuki T., Yokoyama T., Takechi M., Urano H., Yoshida M. and Suzuki T. 2025 *Nucl. Fusion* **65** 016013
[16] Szepesi T. *et al* 2026 *Fusion Eng. Des.* **222** 115530
[17] Yokoyama T. *et al* 2024 *Nucl. Fusion* **64** 126031
[18] Sumida S. *et al* 2026 *Nucl. Fusion* **6** 066023
[19] Réfy D.I. *et al 50th EPS Conf. on Plasma Physics* (*Salamanca, Spain, 8–12 July 2024*) (available at: https://lac913.epfl.ch/epsppd3/2024/html/PDF/P5-073.pdf)
[20] Kaye S.M. *et al* 1997 *Nucl. Fusion* **37** 1303
[21] Ohtani Y. *et al* Confinement property in the JT-60SA first operational phase *Nucl. Fusion* submitted
[22] Goldston R.J. 1984 *Plasma Phys. Control. Fusion* **26** 87
[23] Yushmanov P.N., Takizuka T., Riedel K.S., Kardaun O.J.W.F., Cordey J.G., Kaye S.M. and Post D.E. 1990 *Nucl. Fusion* **30** 1999
[24] Ohtani Y., Yoshida M., Nakano T., Sano R., Wakatsuki T., Inoue S. and Urano H. 2025 *Plasma Phys. Control. Fusion* **67** 055042
[25] Fukumoto M., Nakano T., Wakatsuki T., Kojima S., Ohtani Y., Sano R., Inoue S., Urano H. and Yoshida M. 2025 *Nucl. Mater. Energy* **42** 101816
[26] Tsuchiya K. *et al* 2026 *Nucl. Fusion* **66** 066012
[27] Yamazaki H. *et al* 2025 Results of electron cyclotron heating and current drive system operation in the integrated commissioning phase on JT-60SA *Preprint: 2025 IAEA Fusion Energy Conf.* (*Chengdu*) (available at: https://conferences.iaea.org/event/392/contributions/35826/attachments/19816/36370/IAEA-FEC_yamazaki_20251017F.pdf)
[28] Kayano H. *et al* 2025 Machine enhancement of tokamak device for the JT-60SA next operation *Preprint: 2025 IAEA Fusion Energy Conf.* (*Chengdu*)
[29] Kojima S. *et al* 2025 Optimal design of fast plasma boundary control considering vertical instability features using in-vessel coils in JT-60SA *Preprint: 2025 IAEA Fusion Energy Conf.* (*Chengdu*) (available at: https://conferences.iaea.org/event/392/papers/36395/files/13850-IAEA_Proc_Kojima4.pdf)
[30] Nakano T. *et al 6th Int. Conf. on Frontier in Diagnostic Technologies* (*Frascati, 19–21 October 2022*)
[31] Sozzi C. *et al* 2025 Overview of the European contribution to the diagnostic equipment of jt-60sa for the next operational phases *Preprint: 2025 IAEA Fusion Energy Conf.* (*Chengdu*) (available at: https://conferences.iaea.org/event/392/papers/36327/files/13484-Sozzi%20FEC%202025_v4.pdf)
[32] Loarte A. *et al* 2025 *Plasma Phys. Control. Fusion* **67** 065023
[33] Dumont R. *et al* 2025 West long-pulse achievements in support of next-step fusion devices *Preprint: 2025 IAEA Fusion Energy Conf.* (*Chengdu*)
[34] Song Y. *et al* 2023 *Sci. Adv.* **9** eabq4273
[35] Tani K., Azumi M. and Devoto R.S. 1992 *J. Comput. Phys.* **98** 332
[36] Artaud J.F. *et al* 2018 *Nucl. Fusion* **58** 105001
[37] Garcia J., Hayashi N., Baiocchi B., Giruzzi G., Honda M., Ide S., Maget P., Narita E., Schneider M. and Urano H. 2014 *Nucl. Fusion* **54** 093010
[38] Hayashi N., Garcia J., Honda M., Narita E., Ide S., Giruzzi G. and Sakamoto Y. 2017 *Nucl. Fusion* **57** 126037
[39] Garzotti L. *et al* 2018 *Nucl. Fusion* **58** 026029
[40] Aiba N. *et al* 2025 H-mode operation scenarios in JT-60SA initial research phase predicted by integrated core-pedestal-SOL/divertor simulation *Preprint: 2025 IAEA Fusion Energy Conf.* (*Chengdu*) (available at: https://conferences.iaea.org/event/392/papers/35750/files/13583-Manuscript_FEC2025_Aiba_final.pdf)
[41] Honda M., Aiba N., Seto H., Narita E. and Hayashi N. 2021 *Nucl. Fusion* **61** 116029

[42] Erba M., Cherubini A., Parail V.V., Springmann E. and Taroni A. 1997 *Plasma Phys. Control. Fusion* **39** 261
[43] Snyder P.B., Groebner R.J., Leonard A.W., Osborne T.H. and Wilson H.R. 2009 *Phys. Plasmas* **16** 056118
[44] Saarelma S., Connor J.W., Bilkova P., Bohm P., Field A.R., Frassinetti L., Fridstrom R. and Kirk A. 2023 *Nucl. Fusion* **63** 052002
[45] Kawashima H., Shimizu K., Takizuka T., Sakurai S., Nakano T., Asakura N. and Ozeki T. 2006 *Plasma Fusion Res.* **1** 031
[46] Shimizu K., Takizuka T., Ohya K., Inai K., Nakano T., Takayama A., Kawashima H. and Hoshino K. 2009 *Nucl. Fusion* **49** 065028
[47] Romanelli M. (EFDA-JET Contributors) 2014 *Plasma Fusion Res.* **9** 3403023
[48] Gabriellini S. *et al* 2025 *Nucl. Fusion* **65** 056041
[49] Joffrin E. *et al* Pulse Design Simulator for JT-60SA *Preprint: 2025 IAEA Fusion Energy Conf.* (*Chengdu*) (available at: https://conferences.iaea.org/event/392/papers/35910/files/13860-Joffrin-papier-IAEA2025.pdf)
[50] Kazakov Y.E.O. *et al* 2025 Insights from fast-ion physics studies on JET in support of JT-60SA and ITER Rebaseline *Preprint: 2025 IAEA Fusion Energy Conf.* (*Chengdu*) (available at: https://conferences.iaea.org/event/392/papers/36139/files/13794-Kazakov-FEC2025-v2.pdf)
[51] Coelho R. *et al* 2023 *Front. Phys.* **11** 1267696
[52] Garcia J. (JET Contributors) 2022 *Plasma Phys. Control. Fusion* **64** 104002
[53] Mazzi S. *et al* 2022 *Nat. Phys.* **18** 776–82
[54] Garcia J. *et al* 2024 *Nat. Commun.* **15** 7846
[55] Di Siena A. *et al* 2025 *Nucl. Fusion* **65** 086019
[56] Ruiz Ruiz J. *et al* 2025 *Phys. Rev. Lett.* **134** 095103
[57] Jenko F., Dorland W., Kotschenreuther M. and Rogers B.N. 2000 *Phys. Plasmas* **7** 1904
[58] Iantchenko A. 2024 *Nucl. Fusion* **64** 026005
[59] Coelho R. *et al* Alpha particle generation and confinement in D-^{3}He scenarios in JT-60SA *Nucl. Fusion* submitted
[60] Varje J. *et al* 2019 arXiv:1908.02482
[61] Kazakov Y.E.O. *et al* 2021 *Phys. Plasmas* **28** 020501
[62] Nocente M. *et al* 2021 *Nucl. Fusion* **60** 124006
[63] Rubino G. *et al* Study of the divertor pumping capability in V-Shaped JT-60SA divertor *51th EPS Conf. on Contr. Fusion and Plasma Phys* (*Salamanca, Spain*, *7–11 July 2024*) (available at: https://lac913.epfl.ch/epsppd3/2025/html/PDF/P5_261.pdf)
[64] De Gianni L. *et al* 2024 *Front. Phys.* **12** 1422286
[65] Richou M. *et al* Actively cooled plasma facing components design for W7-X and JT-60SA in support of the ITER divertor *Nucl. Fusion* submitted
[66] Aleixo D.D. *et al* 2025 *Nucl. Mater. Energy* **45** 102030